Journal of Marine Systems 159 (2016) 41–54

Contents lists available at ScienceDirect

Journal of Marine Systems

journal homepage: www.elsevier.com/locate/jmarsys

Geochemical forms and seasonal variations of phosphorus in surface sediments of the East China Sea shelf

Fengxia Zhou [a,c], Xuelu Gao [a,d,*], Huamao Yuan [b], Jinming Song [b], Chen-Tung Arthur Chen [d], Hon-Kit Lui [d], Yong Zhang [a]

[a] Key Laboratory of Coastal Environmental Processes and Ecological Remediation, Yantai Institute of Coastal Zone Research, Chinese Academy of Sciences, Yantai, Shandong 264003, China
[b] Key Laboratory of Marine Ecology and Environmental Sciences, Institute of Oceanology, Chinese Academy of Sciences, Qingdao, Shandong 266071, China
[c] University of Chinese Academy of Sciences, Beijing 100049, China
[d] Department of Oceanography, National Sun Yat-sen University, Kaohsiung 80424, Taiwan

ARTICLE INFO

Article history:
Received 23 December 2015
Received in revised form 8 March 2016
Accepted 10 March 2016
Available online 11 March 2016

Keywords:
Sequential extraction
Sediment analysis
Nutrient geochemistry
Spatial and temporal distribution

ABSTRACT

Geochemical characteristics of phosphorus (P) in the surface sediments of the East China Sea shelf (ECSS) were studied in spring and autumn, 2014. Distributions, seasonal variations, transformations and their influencing factors were discussed. Besides, burial fluxes of P in different seasons were also calculated. Five operationally defined forms of P, namely exchangeable or loosely sorbed P (Ads-P), iron-bound P (Fe-P), authigenic P (Au-P), detrital apatite plus other inorganic P (De-P) and organic P (OP), were obtained using a sequential extraction procedure. Generally, the concentrations of Ads-P, Fe-P, Au-P and OP decreased seaward and the concentrations of De-P increased seaward in both seasons. In spring, the average concentrations of Ads-P, Fe-P, Au-P, De-P and OP were 13.8 ± 5.0, 21.9 ± 7.6, 148.5 ± 44.5, 153.1 ± 55.8 and 91.7 ± 21.5 μg g^{-1}, respectively. The corresponding concentrations in autumn were 11.4 ± 4.3, 20.0 ± 10.9, 170.4 ± 53.6, 225.6 ± 101.7 and 77.1 ± 33.9 μg g^{-1}, respectively. The average percentages of P fractions in total P (TP) in spring and autumn were both in the order: De-P > Au-P > OP > Fe-P > Ads-P. The average concentrations of Bio-available P (Bio-P) were 127.4 ± 31.4 μg g^{-1} in spring and 108.5 ± 47.2 μg g^{-1} in autumn, accounting for 29.8% ± 7.3% and 21.5% ± 8.2% of corresponding TP, respectively. Seasonal variations of the primary production, hydrodynamic conditions, hypoxia and other environmental conditions were responsible for the seasonal variations of different phosphorus forms. The calculation of burial fluxes reflected that, in most parts of the studied area, TP had relative high burial fluxes in autumn, while Bio-P had relatively high burial fluxes in spring. The burial fluxes of other phosphorus forms also showed different seasonal variations in different parts of the studied area.

1. Introduction

Affected by human-induced excessive nutrient input, Chinese coastal environments have experienced eutrophication, frequent occurrence of Harmful Algal Blooms (HABs), elevated productivity and seasonal hypoxia in bottom water in recent decades (Yu et al., 2013; Liu et al., 2015; Xing et al., 2015; Zhou et al., 2008, 2015). Sediment is an important indicator of marine environmental changes (Meyers, 2003; Schelske et al., 1988, 2006; Yu et al., 2013). Phosphorus (P), an important biogenic element, plays an important role in the biological productivity in marine environments (Benitez-Nelson, 2000; Song, 2010; Lui and Chen, 2011; Yu et al., 2012; Samadi-Maybodi et al., 2013; Zhuang et al., 2014). Its cycle is markedly affected by processes taking place in the sediments and at the water–sediment interface (Fisher et al., 1982; Ruttenberg and Berner, 1993; Van Raaphorst and Kloosterhuis, 1994; Föllmi, 1996). Marine sediment not only has a buffering effect on the P concentration in the overlying water, but also is an important source of P in seawater (Giblin et al., 1997; Zabel et al., 1998). According to the study of Fisher et al. (1982), sediments provided 28–35% of P needed in the primary productivity of coastal marine ecosystems.

The East China Sea (ECS) is a typical epicontinental sea (Fig. 1). It has been suffering from environmental deterioration in the rapid industrialization and urbanization of China in the past few decades. Especially since the late 1970s when China's reform and opening up began, a high loading of industrial effluents, agricultural runoff and domestic sewage as well as solid wastes from various human activities were discharged into the ECS (Li and Daler, 2004; Liu et al., 2015). In recent years, much attention has been paid to the P in sediments of different ECS areas, mainly the Changjiang (Yangtze River) Estuary and its adjacent waters owing to the enormous influence of the Changjiang's discharges on the ECS's ecosystem, and a general understanding of its basic geochemistry has been achieved. It has been reported that the total concentrations of P in the surface sediments of the Changjiang

* Corresponding author at: Key Laboratory of Coastal Environmental Processes and Ecological Remediation, Yantai Institute of Coastal Zone Research, Chinese Academy of Sciences, Yantai, Shandong 264003, China.
E-mail address: xlgao@yic.ac.cn (X. Gao).

http://dx.doi.org/10.1016/j.jmarsys.2016.03.005
0924-7963/

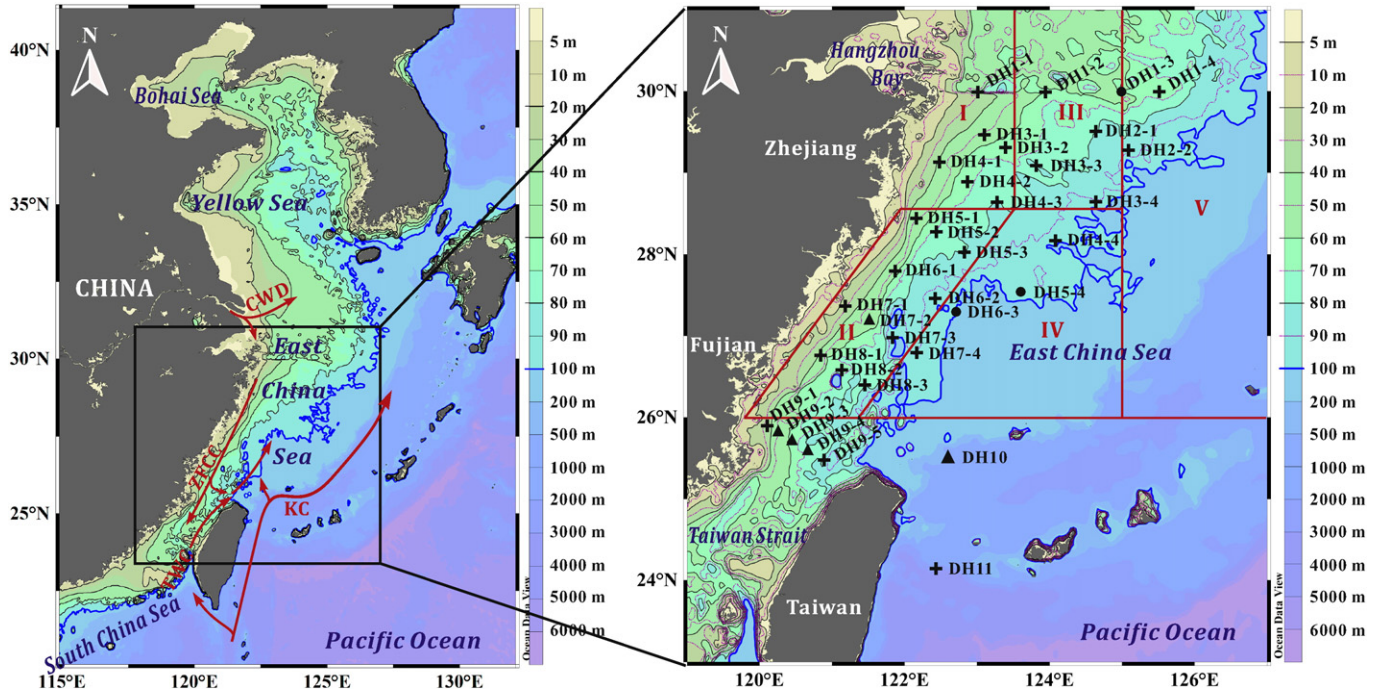

Fig. 1. Locations of sampling sites in the East China Sea shelf. + indicates the locations of sediment samples collected in both spring and autumn; ▲ indicates the locations of sediment samples collected only in spring; ● indicates the locations of sediments samples collected only in autumn. The studied area was divided into five subregions according to the study of Fang et al. (2007): (I) estuary, (II) inner shelf, (III) and (IV) middle shelf, and (V) outer shelf. Based on the principle of proximity, sites DH9-1, DH9-2, DH9-3, DH9-4, and DH9-5 were classified into subregion II and sites DH10 and DH11 were classified into subregion V, respectively. The major currents in the East China Sea are schematically shown. CDW, ZFCC, TWC and KC represent the Changjiang Diluted Water, the Zhejiang–Fujian Coastal Current, the Taiwan Warm Current and the Kuroshio Current, respectively.

Estuary and its adjacent waters varied within a wide range and it existed dominantly in inorganic forms (Fang et al., 2007; Yu et al., 2013; Meng et al., 2014; Yang et al., 2015). The seaward decreasing trends of some P forms revealed their terrestrial origins (Yu et al., 2013; Meng et al., 2014; Yang et al., 2015), and the concentrations of bio-available forms of P (Bio-P) in the northern part of the ECS were slightly lower than in the Yellow Sea (Song and Liu, 2015). The results obtained from the analysis of a sediment core from the ECS inner shelf mud area indicated that the geochemical information of detrital P (De-P) may provide insight into the linkages between regional climate change and flooding events in this region (Meng et al., 2015a).

However, studies on the seasonal variations of P in the surface sediments of the ECS have been largely ignored. The ECS has obvious seasonal variation characteristics, including the seasonal variations of freshwater discharge from coastal rivers, hypoxia outbreak time, nutrient concentrations, chlorophyll *a* (Chl *a*) concentrations, the primary production and so on (Chen et al., 2001, 2004; Rabouille et al., 2008; Wang, 2009; Li et al., 2014). As P has close relations to these parameters, there may be some seasonal variations for P in the surface sediments of the ECS. Besides, knowledge about P in the sediments of the ECS was mainly from the Changjiang Estuary and its adjacent areas, and few studies have focused on P in the sediments of the other parts of the ECS that is relatively far away from the Changjiang Estuary.

Therefore, this study aimed to investigate the concentrations and geochemical fractionations of P in the surface sediments of the ECS shelf (ECSS) generally between 25.5°N and 30°N based on the investigations of two cruises in spring and autumn, to analyze its seasonal variation characteristics and influencing factors, and calculate its burial fluxes.

2. Materials and methods

2.1. Study site and sample collection

The ECSS is bordered by Chinese mainland on the western side (Fig. 1). It is a dynamic system governed by the riverine input and currents (Fig. 1). The Changjiang, the third largest river in the world in its length and runoff, is the major source of materials to the ECSS (Fig. 1). The current system in the ECSS primarily consists of the Changjiang Diluted Water (CDW), the Zhejiang–Fujian Coastal Current (ZFCC), the Taiwan Warm Current (TWC), and the Kuroshio Current (KC) (Zhu et al., 2011) (Fig. 1).

The eco-environment of the ECSS has many obvious seasonal variation characteristics. The discharge of Changjiang is highly seasonal with its peak in summer and 75% of the river runoff occurring during the flood/rainy season between May and October (Rabouille et al., 2008). The hypoxia adjacent to the Changjiang Estuary, which is one of the largest coastal low-oxygen areas in the world (Chen et al., 2007), always occurs in summer and its zone has increased in recent decades (Rabouille et al., 2008; Wang, 2009). Wang et al. (2012) also noted that the increasing trend of hypoxia would continue in next two decades. The primary production in the coastal zone influenced by the Changjiang ranges from 1.5 to 4.5 g C m^{-2} d^{-1} (Chen et al., 2004) during summer. The high primary production is highly seasonal with values falling to 0.04 g C m^{-2} d^{-1} during winter (Chen et al., 2001). The nutrient levels in the Changjiang Estuary and the adjacent area generally peak during autumn and winter (or in early spring), and the lowest value usually occurs in mid-summer which is linked to the phytoplankton growth (Li et al., 2014). The Chl *a* concentrations in the Changjiang River Estuary and the adjacent area are high in summer and low in autumn and winter (Li et al., 2014). The HAB outbreak timing in the ECS has obvious seasonal variation (Li et al., 2014). During the 1980s, the peak of HABs for each year appeared in June to August. However, the frequency peak occurred from May to July in both the 1990s and 2000s (Li et al., 2014).

Sediment samples of this study were collected by a stainless steel box corer during two cruises carried out from May 22–June 11 (spring) and October 18–November 30 (autumn), 2014 on board R/V Science I in the ECSS with water depths generally < 100 m, extending approximately from the east of Zhoushan Archipelago to the north of the Taiwan Strait (Fig. 1). The top ~2 cm sediments were gathered with a plastic spatula

from the center part of the sampler, kept in pre-cleaned polyethylene bags and frozen until lab analysis.

2.2. Analytical methods

We employed the sequential extraction procedure reported in Ruttenberg (1992) to determine different geochemical fractions of P. The five operationally defined forms of P obtained through this scheme were: (i) exchangeable or loosely sorbed P (Ads-P); (ii) iron-bound P (Fe-P); (iii) authigenic P (Au-P); (iv) De-P which is the constituents of detrital apatite plus other inorganic P; and (v) organic P (OP). The inorganic P (IP) in sediments was calculated as the sum of the former four forms of P, and the total P (TP) was the sum of all the P forms.

Freeze-dried samples were thoroughly ground, homogenized and sieved through a 200 mesh screen. Then ~0.1 g of each sample was weighed and loaded into a 50 ml centrifuge tube with 10 ml extraction solutions to perform the sequential extraction scheme. Ads-P was extracted with 1 M $MgCl_2$ (pH = 8.0). Fe-P was extracted with CDB (0.22 M sodium citrate, 0.14 M sodium dithionite, 1.0 M sodium bicarbonate) (pH = 7.6). Au-P was extracted with acetate buffer (pH = 4.0). De-P was extracted with 1 M HCl. Finally, OP in the residual sediment samples was extracted with 1 M HCl after the samples were ashed at 550 °C for 2 h. The detailed sequential extraction protocol has been described by Ruttenberg (1992) and Samadi-Maybodi et al. (2013). The concentration of P was determined by using an inductively coupled plasma optical emission spectrometer (Optima 7000 DV, PerkinElmer, USA) and the analytical conditions followed the report of Gunduz et al. (2011).

The analytical data quality was guaranteed through the implementation of laboratory quality assurance and quality control methods, including the use of standard operating procedures, analysis of reagent blanks, and analysis of replicates. The precision of the analytical procedures was expressed as the relative standard deviation (RSD). The RSD of standard solution was better than 5%; all analyses of samples were carried out in duplicate and the RSDs were less than 3%, and the results were expressed as the mean. Duplicates of 10 samples were also made in the sequential extraction process, and the RSDs were less than 10%. All reagents were analytical or guaranteed grade; all the labwares (bottles, tubes, etc.) were pre-cleaned by soaking in 10% HNO_3 (v/v) for at least 2 days, followed by soaking and rinsing with de-ionized water. Detection limits, three times the standard deviation of 10 replicate measurements of reagent blank, were: 0.011 μg g^{-1} for Ads-P, 0.045 μg g^{-1} for Fe-P, 0.084 μg g^{-1} for Au-P, 0.047 μg g^{-1} for De-P and 0.009 μg g^{-1} for OP.

The sample granulometry was analyzed using a Malvern Mastersizer 2000 laser diffractometer capable of analyzing particle sizes between 0.02 and 2000 μm. The percentages of the following 3 groups of grain sizes were determined: <4 μm (clay), 4–63 μm (silt), and >63 μm (sand). Two aliquots of each freeze-dried, homogenized and ground sample, one treated with 1 M HCl to remove carbonates and the other not, were analyzed with an Elementar vario MACRO cube CHNS analyzer to determine carbon concentration. The result of the aliquot not acid-treated was total carbon (TC) concentration, the result of the acid-treated aliquot was total organic carbon (TOC) concentration, and the total inorganic carbon (TIC) concentration was calculated by subtracting TOC from TC.

3. Results

3.1. General characteristics of sediments

As shown in Fig. 2, the distribution patterns of the grain size fractions in the ECSS are similar in spring and autumn. Fine-grained sediments predominated in the Zhejiang–Fujian coast, while coarser sandy sediments dominated the offshore areas (Fig. 2). The ternary diagram in Fig. 3 categorized the surface sediments of the ECSS according to the classification of Shepard (1954). It shows that the surface sediments of the ECSS were predominantly composed of clayey silt, silt, sandy silt and silty sand; only surface sediments of a few sites were composed of sand (Fig. 3). The percentages of clay and silt fractions ranged from 2.2% to 28.6% with a mean of 15.3% ± 6.6% (mean ± SD) and 5.5% to 78.6% with a mean of 47.4% ± 22.0%, respectively, and the percentages of sand fraction accounted for 0.3–92.4% with a mean of 37.3% ± 28.0% (Fig. 2). The average concentrations of clay and silt fractions in spring and autumn were comparable and did not show obvious seasonal variations (data not shown), while the average concentrations of sand fraction in spring and autumn showed an obvious change, with the average concentration in autumn (39.9% ± 28.6%) about 15% higher than that in spring (34.8% ± 27.5%). In the area where water depth was <100 m, the increase of the average sand fraction in autumn was about 20%.

The TOC concentrations ranged from 0.15% to 0.75% with an average of 0.52% ± 0.14% in spring, and a slightly narrower range of 0.17% to 0.75% with a relatively lower average of 0.43% ± 0.15% recorded for TOC in autumn (Fig. 4a and c). The distribution pattern of TOC in the ECSS was generally similar in the two seasons (Fig. 4a and c), decreasing from the estuarine-inner shelf to the outer shelf. This distribution pattern corresponded to the trend of progressive seaward decline of fine-grained fractions of sediments (silt + clay) (Fig. 2a, b, d and e), which have a larger specific surface area than coarser fraction of sediments (sand), providing them with more binding sites for the adsorption of organic matter (Keil et al., 1994; Mayer, 1994). In summer, a large fraction of particulate organic carbon transported by the Changjiang is deposited off its Estuary; in winter, strong waves disturb the sediments and the southwestward flowing ZFCC (Chen, 2008) moves the particulate organic carbon southwestwards along the Chinese coasts, thus forming the high TOC band (Fig. 4a and c). The TIC concentrations in the ECSS ranged from 0.41% to 2.61% in spring (1.10% ± 0.58% in average) and 0.69% to 2.17% in autumn (1.18% ± 0.38% in average) (Fig. 4b and d). Its distribution patterns in spring and autumn were similar with sand fraction, with relatively low concentrations in the coastal sea areas and relatively high concentrations in the offshore sea areas (Fig. 2c and f; Fig. 4b and d).

3.2. Total P and its forms

In terms of the TP concentrations, their variation range in the surface sediments of the ECSS was from 324.0 to 810.4 μg g^{-1}, which was comparable with or wider to some extent than those reported for the Bohai Sea (322.4–616.9 μg g^{-1}), the Yellow Sea (232.8–768 μg g^{-1}), and the Changjiang Estuary and its adjacent areas (300.7–689.8 μg g^{-1}) (Table 1). Nonetheless, the mean of TP in the ECSS was lower than most of those reported values listed in Table 1. As the dominant component of TP, IP concentrations in the surface sediments of the ECSS had a comparable or wider variation range in contrast with those reported for the other Chinese marine areas listed in Table 1, which was similar to that of the TP, and the mean of IP was lower than that of the Changjiang Estuary and its adjacent areas but higher than those of the Bohai and Yellow Seas.

TP and IP both had obvious seasonal variations, with their average concentrations in autumn obviously higher than that in spring (Table 1). Although the TP and IP concentrations in sediment have been used to indicate the status of increased P input and eutrophication in overlying waters (Schelske and Hodell, 1995; Hodell and Schelske, 1998), it is obvious that the geochemical fractionation of P could provide more environmental information such as potential bioavailability, mobility and provenance than TP and IP do (Yu et al., 2013). Therefore, the results of P based on the sequential extraction analysis will be discussed in the following sections.

3.2.1. Exchangeable or loosely sorbed P

The concentrations of Ads-P in the surface sediments of the ECSS were very low in both spring and autumn compared with the other

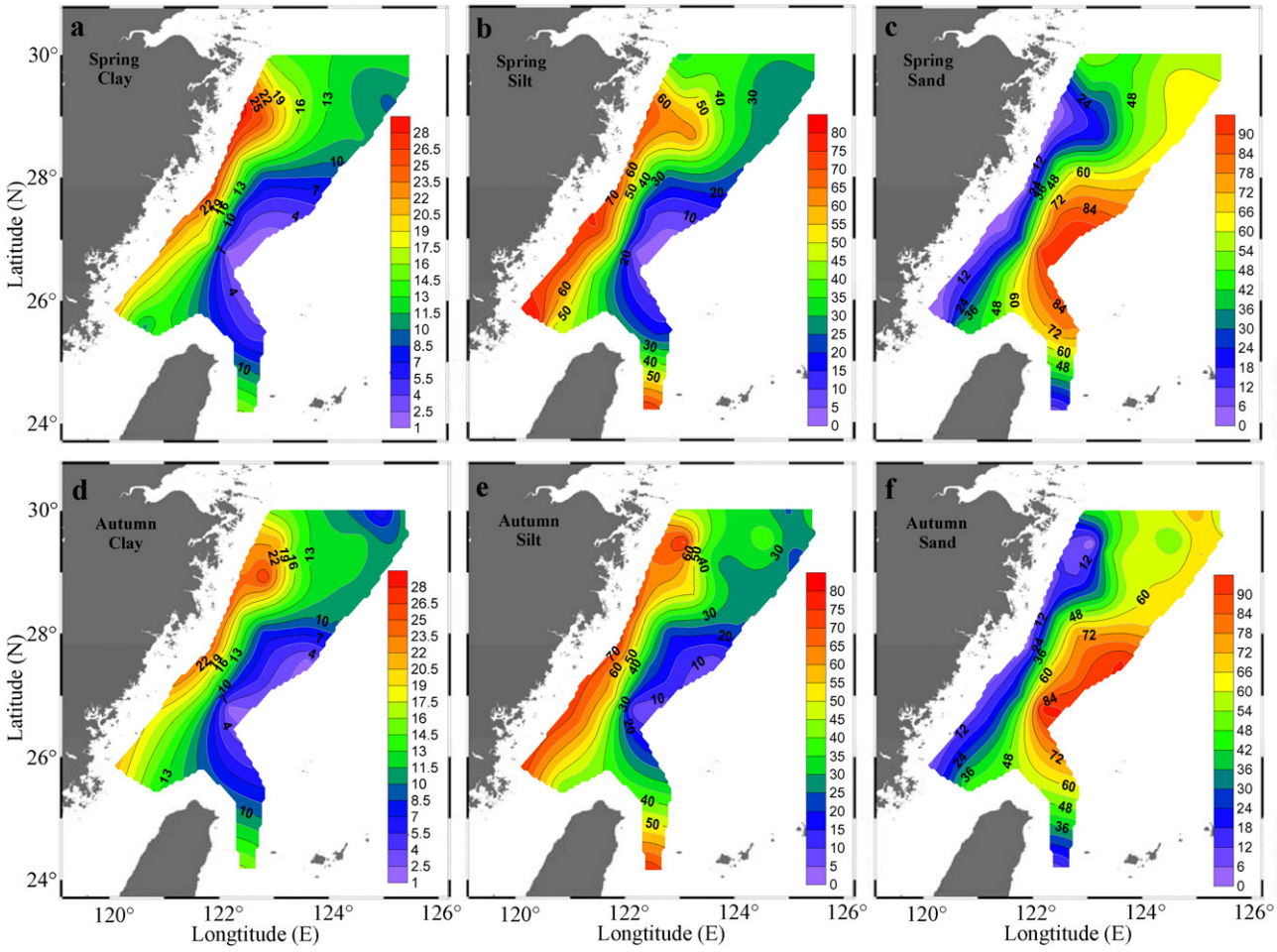

Fig. 2. Spatial variations of clay, silt and sand fractions of sediments in the East China Sea shelf in spring and autumn (unit: %).

forms of P (Table 1). In spring, the concentrations of Ads-P ranged from 0.8 to 21.9 μg g^{-1} with a mean of 13.8 ± 5.0 μg g^{-1}, which only accounted for 0.2–4.9% of the TP concentrations (Table 1 and Fig. 5). In autumn, the concentrations of Ads-P in the ECSS ranged from 5.4 to 20.4 μg g^{-1} with a slightly lower mean Ads-P value of 11.4 ± 4.3 μg g^{-1}, which only accounted for 1.1–3.8% of the TP concentrations (Table 1 and Fig. 5). Although the investigations were carried out in different years and areas of the ECS, the concentrations of Ads-P obtained in this study on the whole corresponded well with the Ads-P values reported in Yu et al. (2013) and Meng et al. (2014) (Table 1).

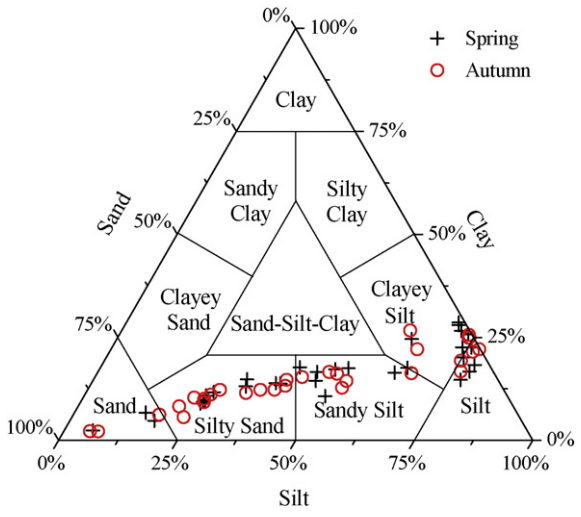

Fig. 3. Ternary diagram showing the Shepard's classification and textures of the surface sediments in spring and autumn.

The spatial distribution patterns of Ads-P indicated that both in spring and autumn high values were recorded in the western strip of the studied area, and decreased gradually seaward (Fig. 6a and b). A distinct difference in the spatial distribution patterns of Ads-P in the two studied seasons was that spring had a much smaller area with a low value of <10 μg g^{-1} than autumn. The differences in the concentrations of P forms between spring and autumn were calculated and plotted in Fig. 7. As shown in Fig. 7a, relatively high concentrations of Ads-P in spring almost occurred in the whole studied area except the areas where the sand fraction was high (Fig. 2c and f).

3.2.2. Fe-bound P

Among the various types of natural particles, iron hydroxides and oxides have the strongest adsorption capacity for P (Berner, 1973; Zhuang et al., 2014). Fe-P percentages of TP were relatively higher than Ads-P (Fig. 5). The concentrations of Fe-P ranged from 7.7 to 36.5 μg g^{-1} accounting for 1.6–8.3% of the TP in spring, and they ranged from 7.6 to 42.2 μg g^{-1} accounting for 1.1–7.9% of the TP in autumn (Table 1 and Fig. 5). Like the spatial patterns of clay, silt and Ads-P, concentrations of Fe-P also decreased seaward (Fig. 6c and d).

The average concentration of Fe-P in spring was comparable with that in autumn (Table 1). However, it presented some distinguishing differences in spatial features between spring and autumn. Relatively higher concentrations of Fe-P occurred in the northern part of the studied area in spring (Fig. 7b), about 60% higher than in autumn. While in

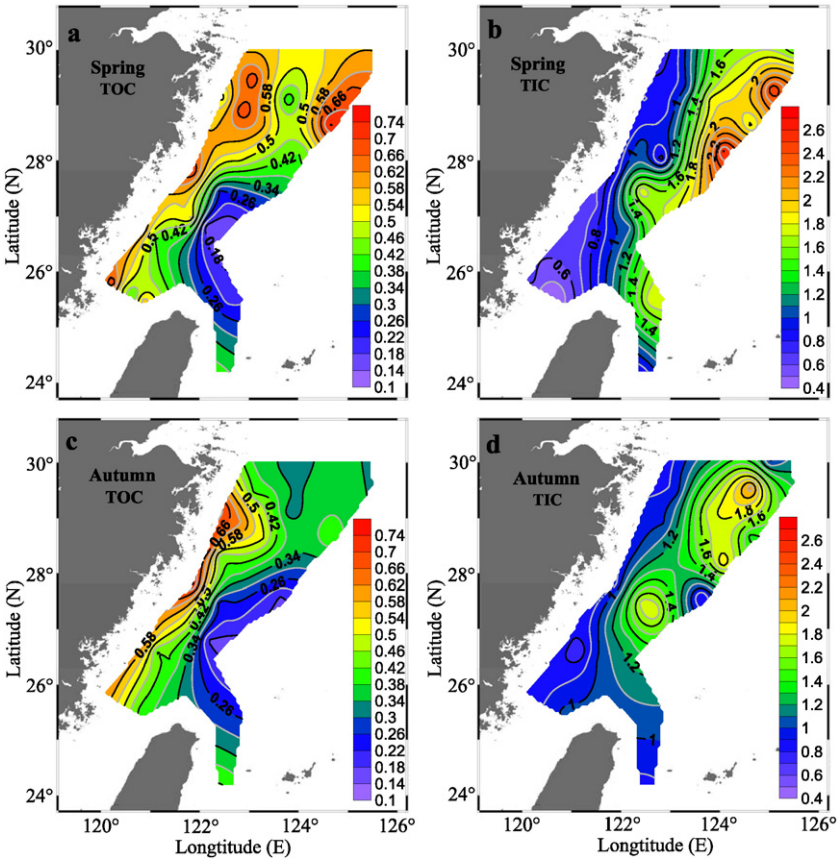

Fig. 4. Spatial variations of TOC and TIC in the surface sediments of the East China Sea shelf in spring and autumn (unit: %).

most of the remaining parts, relatively high concentrations of Fe-P were found in autumn compared with those in spring.

3.2.3. Authigenic P

In spring, the concentrations of Au-P in the ECSS ranged from 28.0 to 250.7 μg g^{-1}, which represented 7.0–56.5% of the TP concentrations (Table 1 and Fig. 5). The concentrations of Au-P in autumn ranged from 60.0 to 332.1 μg g^{-1}, which accounted for 14.1–62.4% of the TP concentrations (Table 1 and Fig. 5). Relatively high concentrations of Au-P were found in the Zhejiang–Fujian coast and the area off northeastern Taiwan where fine-grained sediments were located (Fig. 6e and f; Fig. 2a, b, d and e).

Fig. 7c showed that the concentrations of Au-P in autumn were higher than those in spring in almost the whole studied area except the northern patch. The average concentration of Au-P in autumn was about 15% higher than that in spring (Table 1).

Table 1
Comparison of the concentrations of different geochemical forms of P in the surface sediments of the present study and some other Chinese marginal seas that reported in the literature (μg g^{-1}). It should be noticed that the sequential extraction methods used in the cited literature are not exactly the same as in our research.

Location	Sampling time		TP	IP	Ads-P	Fe-P	Au-P	De-P	OP	Bio-P	Reference
East China Sea shelf	May–Jun., 2014	Range	324.0–499.6	222.8–423.2	0.8–21.9	7.7–36.5	28.0–250.7	94.4–335.4	39.6–131.4	72.4–187.1	This study
		Mean ± SD	429.0 ± 34.3	337.2 ± 38.1	13.8 ± 5.0	21.9 ± 7.6	148.5 ± 44.5	153.1 ± 55.8	91.7 ± 21.5	127.4 ± 31.4	
	Oct.–Nov., 2014	Range	345.1–810.4	293.9–732.1	5.4–20.4	7.6–42.2	60.0–332.1	100.3–488.3	39.6–144.5	57.6–203.2	
		Mean ± SD	504.5 ± 97.3	427.4 ± 88.7	11.4 ± 4.3	20.0 ± 10.9	170.4 ± 53.6	225.6 ± 101.7	77.1 ± 33.9	108.5 ± 47.2	
Changjiang Estuary and its adjacent area	na[a]	Range	418.5–689.8	373.4–594.6	na	na	16.4–54.9	289.9–533.5	33.8–182.3	na	Fang et al. (2007)
		Mean	541.6	456.6	na	na	31.0	380.4	85.2	na	
	2006–2007	Range	300.7–674.3	259.2–590.6	na	na	42.2–135.2	157.8–419.4	23.6–176.1	61.7–301.3	Yang et al. (2015)
		Mean	521.1	422.2	na	na	76.3	275.9	98.6	165.7	
	May, 2009	Range	444.2–672.4	na	6.8–20.7	na	12.0–76.0	216.0–426.0	BDL[b]-11.6	68–250	Yu et al. (2013)
		Mean	552.9	na	13.6	na	46.2	316.4	3.9	na	
	Jul.–Aug., 2011	Range	465.0–663.4	261–486	7.4–29.5	1.6–20.2	16.7–46.5	204.6–409.2	79.4–243.0	44.3–161.2[c]	Meng et al. (2014)
		Mean	527.0	348	13.6	13.3	28.5	293.0	178.7	111.5	
Bohai Sea	1998–1999	Range	322.4–616.9	252.3–523.9	na	na	na	na	21.1–208.0	na	Liu et al. (2004)
		Mean	505.9	400.4	na	na	na	na	105.9	na	
Yellow Sea	1998–1999	Range	232.8–554.9	173.9–480.5	na	na	na	na	7.8–146.6	na	Liu et al. (2004)
		Mean	427.7	351.8	na	na	na	na	76.2	na	
Southwest Yellow Sea	2006–2007	Range	278–768	160–653	na	na	na	na	3.4–267	na	Hong et al. (2010)
		Mean	na	na	na	na	na	na	na	na	

[a] na: not available.
[b] BDL: below detection limit.
[c] A fraction called refractory P was separated from the OP pool in the work of Meng et al. (2014), and the concentrations of Bio-P in their paper did not contain this part of OP.

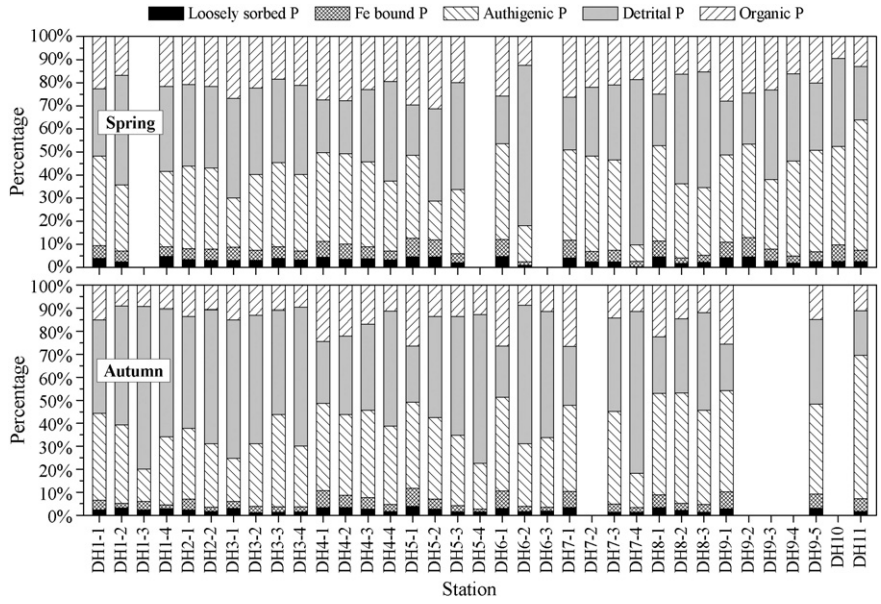

Fig. 5. Distributions of P in different geochemical fractions in the surface sediments of the East China Sea shelf in spring and autumn.

3.2.4. Detrital P

On the whole, De-P was the most abundant form of P in the surface sediments of the ECSS (Fig. 5), and this was consistent with the reports of Fang et al. (2007) and Meng et al. (2014). In spring, the concentrations of De-P ranged from 94.4 to 335.4 μg g^{-1}, which accounted for 20.5–71.7% of the TP with a mean of 35.8%; in autumn, the concentrations of De-P ranged from 100.3 to 488.3 μg g^{-1}, which accounted for 19.6–70.7% of the TP with a mean of 44.3% (Table 1 and Fig. 5). The distribution pattern of De-P was contrary to that of Ads-P, Fe-P, Au-P and OP but similar with that of sand and TIC, with relatively low values in the inshore areas and relatively high values in the offshore areas of the ECSS (Fig. 2c and f; Fig. 4c and d; Fig. 6g and h).

Fig. 7d showed that in most parts of the studied area, the concentrations of De-P in autumn were higher than in spring. This distinguishing feature could also be easily seen from the difference in the average concentrations of De-P between the two seasons, which was 47% higher in autumn than in spring (Table 1).

3.2.5. Organic P

OP was found to be the third dominant form of P after Au-P and De-P, and its contribution to the total P pool was generally less than 30% (Fig. 5). In spring, the concentrations of OP in the surface sediments of the ECSS ranged from 39.6 to 131.4 μg g^{-1}, which accounted for 9.5%–31.2% of the TP; in autumn, its concentrations ranged from 39.6 to 144.5 μg g^{-1}, accounting for 8.9%–26.6% of the TP (Table 1 and Fig. 5). The concentrations of OP in the ECSS were comparable with that in the Changjiang Estuary and its adjacent sea and the Yellow Sea (Table 1; Liu et al., 2004; Fang et al., 2007; Yang et al., 2015). The seaward decreasing spatial pattern was also found for OP in both spring and autumn (Fig. 6i and j).

The average concentration of OP in the surface sediments of the ECSS was higher in spring than in autumn (91.7 ± 21.5 μg g^{-1} in spring and 77.1 ± 33.9 μg g^{-1} in autumn; Table 1). This seasonal difference in OP concentrations was also found in the southwestern Yellow Sea (Hong et al., 2010) and the Bay of Seine (Andrieux and Aminot, 1997). The greatest difference in OP concentrations between the two seasons was found in the northeastern part of the studied area, where the concentrations of OP in spring were about 50% higher than in autumn (Fig. 7e). At the west edge of the studied area, the concentrations of OP were higher in autumn than in spring (Fig. 7e), which was also the case for Fe-P (Fig. 7b).

3.2.6. Bio-available P

Ads-P in the sediment could be easily released into the water and utilized by phytoplankton (Samadi-Maybodi et al., 2013; Zhuang et al., 2014). Fe-P is considered to be an easily resolved constituent of sediments, since it may vary with the change of environmental redox conditions (Samadi-Maybodi et al., 2013; Zhuang et al., 2014). Au-P and De-P have a minor contribution to the accumulation of P in the sediment pore water or overlying water due to their low activities in the weak alkaline aquatic environment (Sagher et al., 1975; Williams et al., 1980; Andrieux and Aminot, 1997). OP is a bio-available form of P (Ruban et al., 2001), because it is biogeochemically active and could mineralize easily to primary producers' usable forms of P (Andrieux and Aminot, 1997; Zhuang et al., 2014).

Consequently, the concentration of Bio-P in the sediment is the sum of the concentrations of Ads-P, Fe-P and OP. The concentrations of Bio-P obtained in this study were comparable with those of previous studies (Table 1; Yu et al., 2013; Yang et al., 2015). In spring, the concentrations of Bio-P in the ECSS ranged from 72.4 to 187.1 μg g^{-1} with a mean of 127.4 ± 31.4 μg g^{-1}, which accounted for 15.0–43.2% of the TP concentrations with a mean of 29.8% ± 7.3%; in autumn, the concentrations of Bio-P ranged from 57.6 to 203.2 μg g^{-1} with a mean of 108.5 ± 47.2 μg g^{-1}, accounting for 12.8%–38.2% of the TP concentrations with a mean of 21.5% ± 8.2% (Table 1 and Fig. 5). The average concentration of Bio-P in spring was 17% higher than that in autumn. Similar seasonal variations of Bio-P could also be found in the study of Andrieux and Aminot (1997). The spatial distribution pattern of Bio-P in both seasons and their seasonal different patterns were most similar to those of the OP (Fig. 6a–d and i–l; Fig. 7a, b, e and f), because, among Ads-P, Fe-P and OP, OP was the dominant composition of Bio-P (Fig. 5).

3.3. Correlation and principal component analysis

Pearson correlation analysis and principal component analysis were performed based on the data in spring and autumn, respectively.

The correlation matrix was shown in Table 2. The correlations for the studied parameters in spring and autumn had both similarities and differences. In both spring and autumn, all P species had significant correlations with clay, silt and sand, with significant positive correlations between De-P and sand, and between other P fractions and clay and silt. This manifested that De-P concentrated in sand fraction, while other P fractions concentrated in clay and silt fractions,

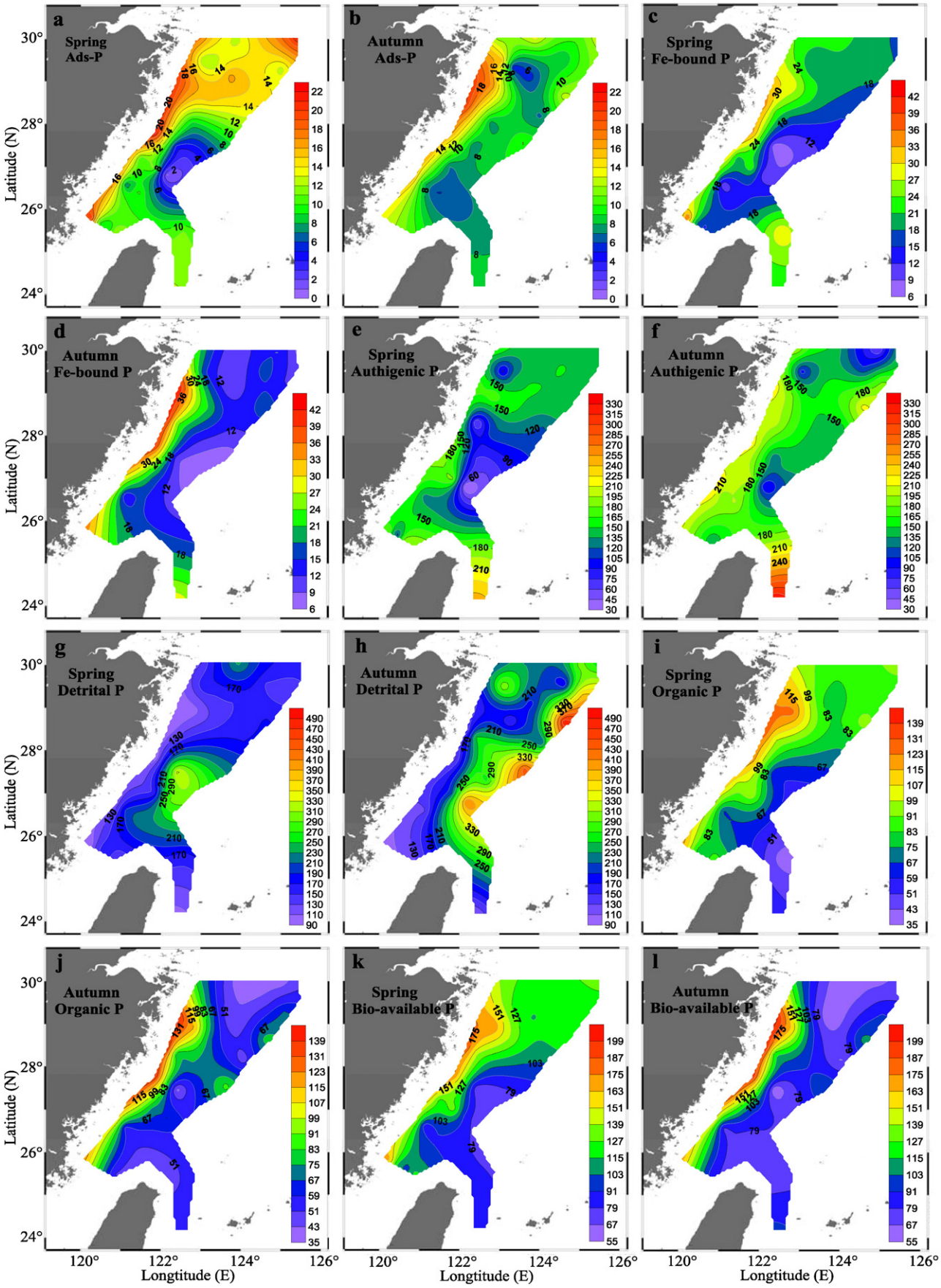

Fig. 6. Spatial variations of P forms in the surface sediments of the East China Sea shelf in spring and autumn (unit: μg g^{-1}).

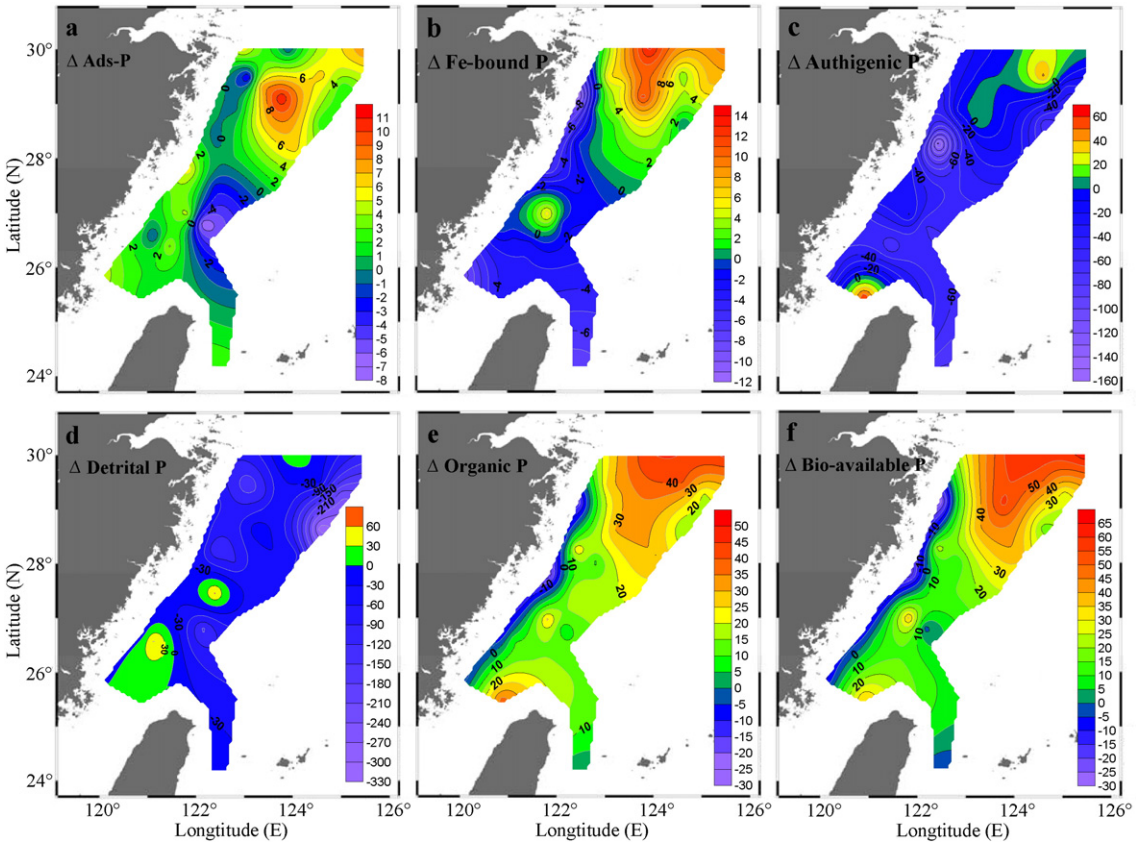

Fig. 7. Spatial distributions of the differences between the concentrations of P forms in spring and autumn (unit: μg g^{-1}).

which were also found in previous studies (Kaiserli et al., 2002; Łukawska-Matuszewska and Bolałek, 2008; Yu et al., 2011, 2013; Meng et al., 2014, 2015a; Zhuang et al., 2014). Ads-P, Fe-P and OP showed significant positive correlations with TOC in both spring and autumn, indicating their common sources. Ads-P showed significant correlations with Au-P and De-P only in spring. Au-P showed significant correlations with OP and TOC only in autumn. The correlations between TIC and Ads-P, Fe-P, Au-P and OP also changed in different seasons. The change of environment conditions between spring and autumn may be responsible for these seasonal variations.

The principal component analysis (PCA), used to study the relationships among measured parameters, facilitates a reduction in data and characterization of a given poly-dimensional system using a small number of new variables (Loska and Wiechuła, 2003). In general, principal components should account for approximately 75% of the total variance (Morrison, 1967), and relevant components are those having eigenvalues >1 (Kaiser, 1960).

In spring, three principal components (PC1–PC3) were identified in the analysis and accounted for 84.3% of the total variance (Fig. 8a and b). Principal component 1 (PC1) accounted for 55.7% of the data variance, and had high positive loadings for the combined variables TOC, Ads-P, Fe-P, Au-P, OP, Bio-P and fine-grained sediments (clay and silt) (Fig. 8a), reflecting the importance of organic matter in the binding of P fractions to fine-grained sediments. These correlations indicated that sources are associated with terrigenous input and anthropogenic activities (Yang et al., 2015). Negative correlations were found between sand and PC1, and De-P and PC1, indicating the absence of organic matter accumulation in this type of sediment. Principal component 2 (PC2) accounted for 17.6% of the total variance, and was characterized by high levels of TP, IP and Au-P. This component showed that IP and Au-P were the dominant species of P in the surface sediments of the ECSS in spring. Principal component 3 (PC3), which explained 11.0% of the total variance, was significantly positive to TIC and significantly negative to silt, indicating the absence of TIC in the silt fraction (Fig. 8b).

Table 2
Pearson correlation matrix for the grain size parameters, TOC, TIC and P species in the sediments of the East China Sea shelf.

		Fe-P	Au-P	De-P	OP	TOC	TIC	Clay	Silt	Sand
Spring	Ads-P	0.796[a]	0.483[b]	−0.780[a]	0.717[a]	0.377[a]	−0.078	0.704[a]	0.496[b]	−0.561[b]
	Fe-P		0.490[b]	−0.759[a]	0.678[a]	0.501[b]	−0.264	0.707[a]	0.580[b]	−0.628[a]
	Au-P			−0.649[a]	0.164	0.282	−0.248	0.448[b]	0.547[b]	−0.541[b]
	De-P				−0.614[a]	−0.635[a]	0.319	−0.717[a]	−0.704[a]	0.729[a]
	OP					0.750[a]	−0.340	0.811[a]	0.534[b]	−0.617[a]
Autumn	Ads-P	0.750[a]	0.314	−0.265	0.794[a]	0.719[a]	−0.521[b]	0.709[a]	0.588[b]	−0.626[a]
	Fe-P		0.598[a]	−0.585[b]	0.873[a]	0.915[a]	−0.517[b]	0.822[a]	0.768[a]	−0.793[a]
	Au-P			−0.448[c]	0.480[b]	0.558[b]	−0.408[c]	0.525[b]	0.604[a]	−0.595[b]
	De-P				−0.314	−0.638[a]	0.237	−0.671[a]	−0.732[a]	0.729[a]
	OP					0.837[a]	−0.548[b]	0.731[a]	0.619[a]	−0.655[a]

[a] $P < 0.001$.
[b] $0.001 < P < 0.01$.
[c] $0.01 < P < 0.05$.

In autumn, two principal components (PC1 and PC2) were distinguished and accounted for 82.1% of the total variance (Fig. 8c). PC1 accounted for 60.1% of the data variance. Like the PC1 in spring, PC1 in autumn also had high positive loadings for the combined variables TOC, Ads-P, Fe-P, Au-P, OP, Bio-P and fine-grained sediments (clay and silt) (Fig. 8c), indicating the importance of organic matter in the binding of P fractions to fine-grained sediments which was a common phenomenon in different seasons. In autumn, PC2 accounted for 22.0% of the data variance and was characterized by high levels of TP, IP and De-P.

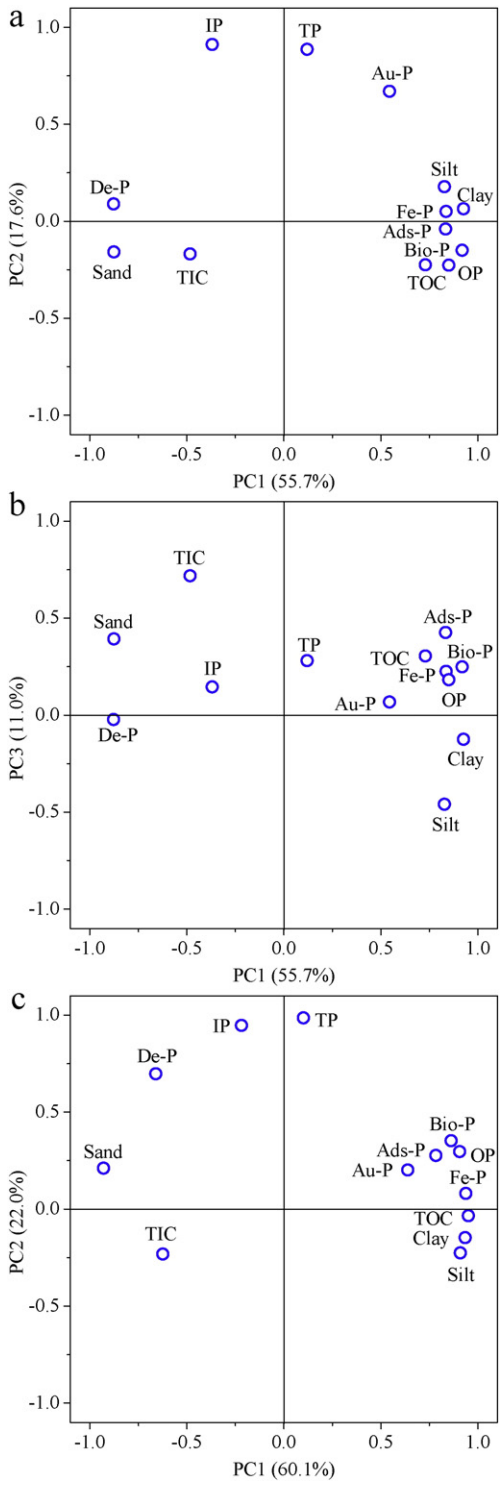

Fig. 8. Loading plots of the measured parameters in the domain defined by two components: PC1 versus PC2 and PC3 in spring, and PC1 versus PC2 in autumn.

This component showed that IP and De-P were the dominant species of P in the surface sediments of the ECSS in autumn, which was somewhat different from that of PC2 in spring.

4. Discussion

4.1. Relationships between primary production and seasonal variations of phosphorus

The nutrient input from the Changjiang fuels high primary production in the adjacent coastal zone in spring and summer (Chen et al., 2001, 2004; Rabouille et al., 2008; Li et al., 2014). It was reported that high primary production could result in high concentrations of particulate OP (Liu et al., 2001; Chai et al., 2006; Yu et al., 2012) and sedimentary OP (Andrieux and Aminot, 1997; Fang, 2000; Dunne et al., 2007; González-Alcaraz et al., 2012; Li et al., 2014; Shao et al., 2014). As a result, relatively high OP concentrations occurred in surface sediments of the northern part of the studied area in spring (Fig. 6i).

Some of OP in surface sediments does not accumulate for long periods (Andrieux and Aminot, 1997) and it can be partially biologically utilized by mineralization and enzymatic hadrolysis (Rydin, 2000; Zhang et al., 2008; Huo et al., 2011; Shao et al., 2014). Besides, the primary production in autumn is low (Rabouille et al., 2008) and therefore low OP can be produced during autumn (Andrieux and Aminot, 1997). This is the reason why the concentrations of OP were generally lower in autumn than in spring (Fig. 7e).

Among the three forms of Bio-P (Ads-P, Fe-P and OP), Ads-P is undoubtedly the most labile form (Andrieux and Aminot, 1997). Ads-P in the sediment can be easily released into water and utilized by phytoplankton (Chen et al., 2011; Samadi-Maybodi et al., 2013; Shao et al., 2014; Zhuang et al., 2014). Reynolds (1976) indicated that owing to the limited nutrient availability in the surface water after the consumption by phytoplankton during summer, phytoplankton tended to grow in deeper waters where nutrients were relatively abundant due to sediment release. Jiang et al. (2008) also pointed out that organisms at the bottom waters could stimulate P release from sediments. The depths of the studied area were generally less than 100 m (Fig. 1). As a result, organisms could easily reach the bottom waters in the studied area. The utilization of P by organisms in deep waters (or bottom waters), which could cause P release from sediments, may be the reason why the concentrations of Ads-P in the surface sediments of the ECSS were generally lower in autumn than in spring.

4.2. Relationships between summer hypoxia and seasonal variations of phosphorus

Previous studies showed that the decomposition of organic matter fueled hypoxia in the Changjiang coastal zone, while the sources of these organic matters were still under debate (Chen et al., 2007; Wei et al., 2007; Rabouille et al., 2008). High concentrations of organic matter usually accompanied high concentrations of OP (Andrieux and Aminot, 1997). Seasonal variation of OP in this study could provide some useful information to that debate.

Hypoxia occurs when oxygen consumption from the decomposition of organic matters exceeds the replenishment of oxygen (Rabouille et al., 2008). Wang et al. (2012) reported the annual cycle of hypoxia off the Changjiang Estuary. The hypoxia begins to develop in late spring and early summer, reaches its maximum in August, weakens in the autumn and finally disappears in the winter (Wang et al., 2012). The latitudinal location of the DO minimum can reach 27°N (Wang et al., 2012). The relatively high OP concentrations in the northern part of the studied area (north of 27°N) in spring did not occur in autumn (Fig. 6i and j). This means that a proportion of OP (about 30%) in the surface sediment of that area was decomposed during late spring and summer when the hypoxic zone was formed and enlarged. Therefore, it could be inferred that the decomposition of organic matter in the northern part of the

studied area was responsible for the formation of the hypoxic adjacent to the Changjiang Estuary. Besides the consumption of oxygen from the organic matter decomposition, physical forcings (stratification, circulation pattern in the region and residence time of the water in the mixing zone) which limit oxygenation of bottom waters were also important factors in the formation of hypoxic off the Changjiang Estuary (Wei et al., 2007; Rabouille et al., 2008; Wang, 2009). In late spring, the combination of high CDW runoff, TWC and strong solar radiation made a strong stratification in the northern ECSS (Wang, 2009). The decomposition of organic matter consumed oxygen, while oxygen could not be replenished due to the strong stratification in late spring. Then, the hypoxic condition was formed in late spring, and enlarged in summer due to stronger stratification (Wang, 2009). Among the conditions which resulted in hypoxia, the decomposition of organic matter in the surface sediment was obviously the direct reason for the formation of the hypoxic condition adjacent to the Changjiang Estuary.

A similar seasonal variation of Fe-P was also found in the northern part of the studied area, with obvious decrease of Fe-P in autumn compared with that in spring (Fig. 6c and d; Fig. 7b). According to the study of Zhou et al. (2001), Fe-P can be released from the surface sediment when anoxic conditions prevail at the sediment–water interface. The hypoxia adjacent to Changjiang Estuary may ultimately lead to anoxia where oxygen completely disappears (Rabouille et al., 2008). Therefore, the summer hypoxia adjacent to the Changjiang Estuary was responsible for the decrease of Fe-P in the northern part of the studied area. Similar seasonal variations of Fe-P and similar influencing factors could also be found in the study of Andrieux and Aminot (1997).

4.3. Relationships between hydrodynamic conditions and seasonal variations of phosphorus

The Changjiang is the third largest in the world (~6300 km in length), and the annual sediment discharge has been reported as ~-4.8×10^8 metric tons, which is ranked the fourth globally (Milliman and Meade, 1983). About 40% of the sediments are trapped in the estuary, and the rest are transported into the neighboring continental shelf of the East China Sea (Milliman et al., 1985; Shen, 2001). It is generally agreed that most of the Changjiang-derived sediments are carried southward along the Zhejiang–Fujian coast under the influence of southward-flowing coastal currents (ZFCC) and deposited west of 123°E because of the barrier effect of the northward flowing Taiwan Warm Current (Milliman et al., 1985; Liu et al., 2010). Relatively high concentrations of Ads-P, Fe-P and OP were found in the inner continental shelf of the East China Sea (west of 123°E) in both spring and autumn (Fig. 6a–d, i and j). This indicated that they were mainly of terrestrial origin. Similar conclusion were also drawn in previous studies (Ruban et al., 2001; Yu et al., 2013; Shao et al., 2014; Meng et al., 2015b). The offshore areas of the ECSS with relatively low concentrations of Ads-P, Fe-P and OP in the surface sediments may result from the relatively weak influence of the CDW and the ZFCC but relatively strong influence of the TWC and KC (Fig. 1; Fig. 6a–d, i and j).

Summer and autumn are the rainy seasons for the southeastern China (Rabouille et al., 2008; Wang and Ding, 2008). Strong rainfall could cause strong surface runoff and then much terrigenous materials could be brought into the coastal area of the ECSS. Therefore, seasonal variations of terrigenous materials in the surface sediment of that area could be expected. The concentrations of Fe-P in the southern part of the studied area were generally higher in autumn than in spring and the largest increase of Fe-P in autumn was found in the coast of the ECSS (DH4-1, Fig. 1; Fig. 7b). There was also an obvious increase of OP in autumn in the coast of the ECSS (Fig. 7e). These phenomena confirmed our expectation that strong rainfall during summer and autumn could influence the seasonal variation of phosphorus fractions in the coast of the ECSS.

Strong resuspension of surface sediment occurred in autumn and winter in the East China Sea (Yu et al., 2012; Li et al., 2014). This hydrological process is likely a factor that changed the sediment grain size composition in autumn compared with spring in the ECSS, for our data indicated that the average percentage of sand fraction sediment in autumn in relative shallow waters (<100 m) was obviously higher than that in spring (34.4% ± 26.7% in spring and 41.1% ± 28.4% in autumn; Fig. 2c and f). As aforementioned, De-P concentrated in coarse sediments, which meant that the coarser the sediments were, the higher concentrations of De-P the sediments had. Therefore, it is understandable that the average concentration of De-P in the surface sediments of the ECSS in autumn was higher than in spring. Meng et al. (2015a) reported that the peak concentrations of De-P in the core sediments of the ECS inner shelf corresponded well with the worst flooding events of the Changjiang in the history. This means that increased rainfall, which always leads rivers into flooding, could result in the increase of De-P concentrations in sediments owing to the fluvial transport of terrestrial matter. Therefore, the increase of De-P concentrations in the surface sediments of the ECSS in autumn may also be partially related to the influence of strong precipitation in summer and autumn in southeastern China.

4.4. Transformation of phosphorus

The molar ratio of TOC to OP (TOC/OP) in marine sediments can reflect the influence of terrestrial organic matter inputs (Redfield et al., 1963; Ruttenberg and Goñi, 1997; Meng et al., 2014). Generally, carbon-to-P content ratios of terrestrial plants are much higher than those of the marine primary producers (Wang et al., 2010; Sardans et al., 2012). According to the study of Ruttenberg and Goñi (1997), TOC/OP higher than the Redfied ratio, i.e. 106 (Redfield et al., 1963), are usually attributed to the dominance of terrestrial sources. In addition, it has been reported that preferential regeneration of P relative to carbon also could lead to this (Ingall and Jahnke, 1997; Schenau and de Lange, 2001; Sekula-Wood et al., 2012). In this study, the spatial distribution of TOC/OP indicated that, in both seasons, most parts of the studied area (except the area where sand fraction was high) had higher values of TOC/OP (>120) (Fig. 9a and c). The evidence in Xing et al. (2011) and Li et al. (2012) suggests that organic matter in sediments of the ECSS were mainly marine-derived. Therefore, preferential loss of P relative to carbon during organic matter decomposition, which was also supported by the evidence in Meng et al. (2014), seems more responsible for the spatial distribution feature of the higher TOC/OP values occurring in most parts of the studied area. The values of TOC/OP in the surface sediment of the ECSS were in the ranges of 52–205 in spring and 52–238 in autumn with the mean of 148 ± 28 and 154 ± 41, respectively. As mentioned in the previous parts, relatively low mean values of TOC and OP were recorded in autumn compared with spring. It could be concluded that the extent of preferential loss of P relative to carbon during organic matter decomposition in the ECSS sediment was greater in autumn than in spring.

As reported, TOC/OP ratios of marine phytoplankton are close to the Redfield ratio 106 (Redfield et al., 1963). If the sedimentary phytoplankton could not be degraded, the TOC/OP ratios in marine surface sediments should also be close to 106. However, part of organisms could be degraded during their settlement or during the short periods after their settlement (Andrieux and Aminot, 1997; Meng et al., 2014). Therefore, a wide range of TOC/OP values was found in the marine surface sediments (Meng et al., 2014; Fig. 9a and c). As OP could be more bioavailable after its mineralization (Andrieux and Aminot, 1997), Ads-P and/or Fe-P may be produced if the mineralized P was not released into water column directly. According to previous studies, nutrient concentrations peak in autumn and winter when Chl *a* concentrations are low (Li et al., 2010; Li et al., 2014). This phenomenon indicates that the mineralized P in sediments could be stored for some time and that kind of P may be Ads-P and/or Fe-P. That is to say, the ratio of TOC/Bio-P in marine surface sediments which has many newly settled organisms may be more close to the Redfield ratio than the ratio of TOC/OP. As

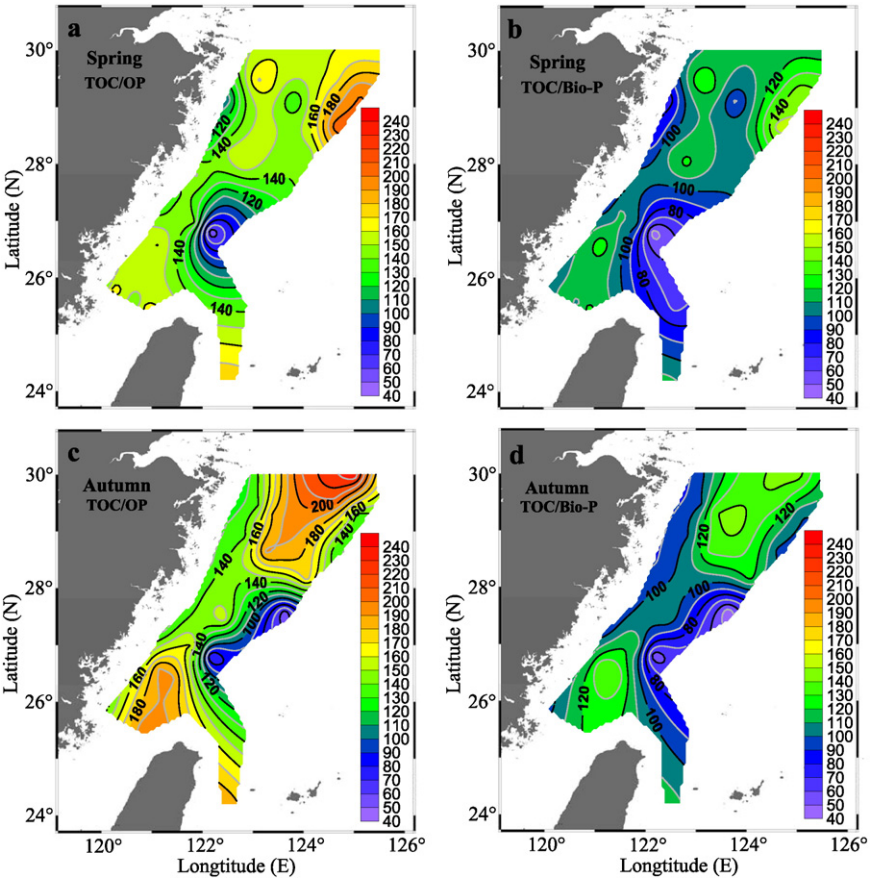

Fig. 9. Spatial distributions of TOC/OP and TOC/Bio-P molar ratios in the surface sediments of the East China Sea shelf in spring and autumn.

a result, TOC/Bio-P ratio was calculated in this study to compare with TOC/OP ratio. In spring, TOC/Bio-P ratios ranged from 45 to 154, with an average value of 106 ± 21; in autumn, TOC/Bio-P ratios ranged from 43 to 145, with an average value of 108 ± 25 (Fig. 9b and d). Compared with the ratios of TOC/OP in spring and autumn and TOC/Bio-P in autumn in this study, the ratios of TOC/Bio-P in spring in most parts of the studied area were relatively close to the Redfield ratio (Fig. 9). This result generally agreed with our expectation. Therefore, it could be deduced that a proportion of OP could degrade into Ads-P and/or Fe-P and some of these newly derived P could be stored in the sediment in spring; in autumn, these newly derived P could be partly released into water column. This deduction was also in agreement with our aforementioned viewpoint that Ads-P could be released into water in autumn due to the utilization of P by organisms. The increase of Fe-P in autumn in the southern part of the studied area may be partly related to the transformation of OP (Fig. 7b and e).

Au-P is composed of things like biological apatite (including bones, teeth, she fragments), $CaCO_3$ incorporated phosphate and carbonate fluorapatite precipitating from interstitial solutions (Sekula-Wood et al., 2012; Samadi-Maybodi et al., 2013). The ECSS is an important fishery and mariculture area in China (Yang et al., 2015). High Au-P concentrations likely originated from the detritus of marine organisms (Zhuang et al., 2014; Yang et al., 2015). Compared with the primary production in spring and summer, the primary production in autumn in the ECSS was relatively low (Rabouille et al., 2008) which indicated mass mortality of organisms in autumn. The settlement of large quantities of biogenic skeletal debris may partly contribute to the increase of Au-P in autumn (Table 1; Fig. 7c). The average concentration of OP in spring was about 20% higher than that in autumn (Table 1). According to previous studies, phosphate derived from OP may precipitate into Au-P (Cha et al., 2005; Fang et al., 2007; Meng et al., 2015a). This manifested that besides the direct settlement of biogenic skeletal debris, the transformation of OP which was produced during spring and summer was another source for the increase of Au-P in autumn. The significant positive correlations between Au-P and OP, and Au-P and TOC in autumn, which were different from that in spring (Table 2), could also support this viewpoint.

Considering the aforementioned information that part of OP could degrade into Ads-P and Fe-P in spring and part of Au-P was derived from OP in summer and autumn, we deduced that part of OP was firstly transformed into Ads-P and Fe-P and later Au-P was formed. Meng et al. (2014) also pointed out that Au-P had relatively slow formation rate.

Based on the above analysis, the integrated situation about the seasonal variations of P fractions in the ECSS could be concisely described as follows. In most parts of the ECSS, relatively high primary production resulted in generally high concentrations of sedimentary OP in spring. Some of the newly derived OP decomposed into Ads-P and/or Fe-P in a short time, which could be stored in sediment over a certain period of time. Compared with the total amount of OP deposited in spring, the amount of OP which could be decomposed in a short time was relatively small. Most of the newly deposited OP was decomposed during late spring and summer, leading to an obvious decrease of sedimentary OP in autumn. The sedimentary OP mineralization during late spring and summer needed much oxygen. However, the northern part of the studied area became stratified in late spring and summer and the oxygen could not be completely replenished, leading to hypoxia in bottom waters and surface sediments. Some of Fe-P could be reduced and transformed into other forms of P, which was the reason for the decrease of Fe-P in autumn in the northern part of the studied area. Owing to the limited nutrient availability in the surface water after the consumption by phytoplankton during summer, phytoplankton tended to grow in deeper waters where nutrients were relatively abundant due to

sediment release. Therefore, some of Ads-P could be released in order to keep balance with the P in water column, thus resulting in generally low concentrations of Ads-P in autumn. Au-P increased in autumn because of the direct settlement of biogenic skeletal debris and the transformation of OP. De-P also increased in autumn, which could be derived from the strong surface sediment resuspension in autumn in the ECSS or the strong precipitation in summer and autumn in southeastern China. The relatively high concentrations of Fe-P and OP in autumn in the coastal areas of the ECSS could also be related to the strong precipitation in summer and autumn in southeastern China.

4.5. Burial fluxes

Previous studies calculated the burial fluxes (BF) of P usually based on the P concentrations from one cruise or the average concentrations from several cruises (Fang et al., 2007; Song and Liu, 2015; Yang et al., 2015). From the results obtained in this study, different P fractions and total P all had obvious seasonal variations and these variations were different in different P fractions and different parts of the studied area (Table 1; Fig. 7). Previous calculated BF cannot reflect the BF information for P in different seasons. Therefore, we attempted to calculate the BF of different P (BF_i) in different seasons and different parts of the studied area to get more knowledge about the BF of P in the ECSS.

The BF_i (μg cm^{-2} yr^{-1}) were generally calculated based on the following formula (Ingall and Jahnke, 1994; Fang et al., 2007; Yang et al., 2015):

$$BF_i = C_i \times \omega$$

where C_i (μg g^{-1}) is the concentrations of different P fractions in surface sediments, and ω (g cm^{-2} yr^{-1}) is the sediment mass accumulation rate. Based on the work of Huh and his colleague (Huh and Su, 1999; Su, 2000; Su and Huh, 2002), Fang et al. (2007) divided the ECSS into five subregions according to the reported ω data and gave the average value of ω in each subregion (Table 3). As shown in Fig. 1, subregion I is estuary area, subregion II is inner shelf area, subregions III and IV are middle shelf area and subregion V is outer shelf area (Fang et al., 2007). Given that the sediment mass accumulation rate in spring and autumn in this study could not be obtained for limited data and the studied area of Fang et al. (2007) was similar with this study, we divided the studied area in this study into five subregions according to Fang et al. (2007) and assumed that the ω in spring and autumn in each subregion were equal to that of Fang et al. (2007). Based on the principle of proximity, sites DH9-1, DH9-2, DH9-3, DH9-4 and DH9-5 were classified into subregion II and sites DH10 and DH11 were classified into subregion V, respectively. Then, we used the average ω in each subregion (Fang et al., 2007; Table 3) and the average P concentrations in each subregion obtained in this study to calculate the BF_i. The BF of TP (BF_{TP}) was also calculated for the comparison with previous data.

Table 3 shows the values of the parameters used in the calculation and the calculated results. Taking the spring and autumn as a whole, the calculated values of the BF for TP in the subregions I–V were 370.4, 137.5, 163.5, 120.7 and 36.0 μg cm^{-2} yr^{-1}, respectively, which were comparable with the data reported by Fang et al. (2007). On average, the BF for TP in the whole studied area in autumn was about 20% higher than that in spring. In both spring and autumn, the BF of different P forms in subregion I all had the highest values compared with that of other subregions (Table 3), which were mainly due to the highest ω in that subregion (Table 3). The average concentration of Ads-P in each subregion decreased in autumn compared with that in spring, resulting in the decrease of $BF_{Ads\text{-}P}$ in each subregion in autumn (Table 3). The BF of Fe-P decreased in most parts of the ECSS in autumn, except the Zhejiang–Fujian coast (Table 3), reflecting that in autumn relatively high concentrations of Fe-P were transported and then settled down in that area. The BF of Au-P increased obviously in subregions I, II and IV in autumn and did

Table 3
Mass accumulation rate (ω), concentrations of P, and corresponding burial flux for each subregion of the East China Sea shelf.

Time	Subregion	ω[a]	$C_{Ads\text{-}P}$	$C_{Fe\text{-}P}$	$C_{Au\text{-}P}$	$C_{De\text{-}P}$	C_{OP}	$C_{Bio\text{-}P}$	C_{TP}	$BF_{Ads\text{-}P}$	$BF_{Fe\text{-}P}$	$BF_{Au\text{-}P}$	$BF_{De\text{-}P}$	BF_{OP}	$BF_{Bio\text{-}P}$	BF_{TP}
		(g cm^{-2} yr^{-1})	(μg g^{-1})	(μg g^{-1})	(μg g^{-1})	(μg g^{-1})	(μg g^{-1})	(μg g^{-1})	(μg g^{-1})	(μg cm^{-2} yr^{-1})	(μg cm^{-2} yr^{-1})	(μg cm^{-2} yr^{-1})	(μg cm^{-2} yr^{-1})	(μg cm^{-2} yr^{-1})	(μg cm^{-2} yr^{-1})	(μg cm^{-2} yr^{-1})
Spring	I	0.8	15.8	24.1	149.1	131.5	106.7	146.6	427.2	12.6	19.3	119.3	105.2	85.4	117.3	341.8
	II	0.3	13.6	22.8	150.4	149.0	95.2	131.6	431.0	4.1	6.8	45.1	44.7	28.6	39.5	129.3
	III	0.35	14.5	20.0	148.6	177.0	85.8	120.3	446.0	5.1	7.0	52.0	62.0	30.0	42.1	156.1
	IV	0.25	9.2	18.9	143.8	179.5	62.0	90.1	413.4	2.3	4.7	36.0	44.9	15.5	22.5	103.4
	V	0.075	16.8	18.2	140.6	149.1	89.9	124.9	414.6	1.3	1.4	10.6	11.2	6.7	9.4	31.1
Autumn	I	0.8	13.2	23.4	162.2	210.5	89.4	126.0	498.7	10.5	18.7	129.8	168.4	71.5	100.8	399.0
	II	0.3	12.3	25.4	191.2	174.2	91.8	129.4	494.8	3.7	7.6	57.4	52.3	27.5	38.8	148.4
	III	0.35	10.0	13.4	138.3	272.9	49.6	73.0	484.1	3.5	4.7	48.4	95.5	17.4	25.5	169.4
	IV	0.25	8.5	13.6	168.5	285.4	62.5	84.6	538.5	2.1	3.4	42.1	71.4	15.6	21.2	134.6
	V	0.075	11.6	10.0	155.2	311.5	57.4	79.1	545.8	0.9	0.8	11.6	23.4	4.3	5.9	40.9
Average	I	0.8	14.4	23.8	155.7	171.0	98.1	136.3	463.0	11.6	19.0	124.6	136.8	78.5	109.0	370.4
	II	0.3	13.1	23.9	167.9	159.8	93.8	130.7	458.4	3.9	7.2	50.4	47.9	28.1	39.2	137.5
	III	0.35	12.0	16.3	142.9	230.3	657	94.0	467.2	4.2	5.7	51.0	80.6	23.0	32.9	163.5
	IV	0.25	8.8	15.9	157.6	238.3	62.3	87.0	482.9	2.2	4.0	39.4	59.6	15.6	21.8	120.7
	V	0.075	14.2	14.1	147.9	230.3	73.7	102.0	480.2	1.1	1.1	11.1	17.3	5.5	7.6	36.0

[a] Data taken from Fang et al. (2007).

not show obvious seasonal variations in subregions III and V, indicating that relatively high biodetritus were produced and settled down in autumn in the inshore areas of the ECSS. The BF of De-P increased obviously in all the subregions in autumn, which was caused by the increase of average De-P concentration in each subregion. The BF of OP decreased obviously in subregions I, III and V in autumn, but did not show clear seasonal variations in subregions II and IV. The BF of Bio-P, i.e. the sum of Ads-P, Fe-P and OP, showed similar seasonal variations with the BF of OP. Generally, the BF of different P forms showed different seasonal variations in the ECSS.

5. Conclusions

Previous studies focused on the concentrations, compositions, spatial distributions and controlling factors of phosphorus (P) in the East China Sea. In this study, we analyzed the seasonal variations of P in the surface sediments of the East China Sea shelf (ECSS).

The concentrations of total P in the surface sediments of the ECSS ranged from 324.0 to 499.6 μg g^{-1} in spring and ranged from 345.1 to 810.4 μg g^{-1} in autumn, which were comparable with those reported for the Bohai Sea, the southwestern Yellow Sea, and the Changjiang Estuary and its adjacent areas. The average concentration of total P in autumn (504.5 ± 97.3 μg g^{-1}) was 17% higher than that in spring (429.0 ± 34.3 μg g^{-1}).

Generally, the concentrations of Ads-P, Fe-P, Au-P and OP decreased seaward and the concentrations of De-P increased seaward in both seasons. In spring, the average concentrations of Ads-P, Fe-P, Au-P, De-P and OP were 13.8 ± 5.0, 21.9 ± 7.6, 148.5 ± 44.5, 153.1 ± 55.8 and 91.7 ± 21.5 μg g^{-1}, respectively. The corresponding concentrations in autumn were 11.4 ± 4.3, 20.0 ± 10.9, 170.4 ± 53.6, 225.6 ± 101.7 and 77.1 ± 33.9 μg g^{-1}, respectively. In both spring and autumn, the percentages of P fractions in TP were in the order: De-P > Au-P > OP > Fe-P > Ads-P. The average concentrations of Bio–P were 127.4 ± 31.4 μg g^{-1} in spring and 108.5 ± 47.2 μg g^{-1} in autumn, accounting for 29.8% ± 7.3% and 21.5% ± 8.2% of corresponding TP, respectively. Correlation and principle component analysis showed that there were both similarities and differences for the relations among parameters studied in different seasons.

Concentrations of Ads-P were generally higher in spring than in autumn. In autumn, phytoplankton tended to utilize P in bottom waters, which could cause the release of P from sediment. This may be responsible for the seasonal variations of Ads-P in the surface sediments of the ECSS. The seasonal variation of Fe-P in the ECSS was complex. Terrestrial inputs, summer hypoxia and transformations of P contributed to that phenomenon. The increase of Au-P in the ECSS in autumn was related to the transformation of P and the settlement of biogenic skeletal debris. Strong resuspension of surface sediment in autumn in the ECSS and the strong precipitation in summer and autumn in southeastern China may be responsible for the increase of De-P concentrations in autumn in the ECSS. Seasonal variations of the primary production, summer hypoxia, terrestrial inputs and transformation of P were responsible for the seasonal variations of OP in the surface sediments of the ECSS.

Burial fluxes calculation manifested that total P generally had high burial fluxes in autumn, while Bio-P generally had high burial fluxes in spring. The burial fluxes of different P forms had different seasonal variations in different parts of the studied area.

Acknowledgments

This study was supported by the Strategic Priority Research Program of the Chinese Academy of Sciences (XDA11020102). The assistance of Baoxiao Qu, Changfeng Qu, Qidong Wang and Jiulong Zuo in the sample collection is greatly appreciated.

References

Andrieux, F., Aminot, A., 1997. A two-year survey of phosphorus speciation in the sediments of the Bay of Seine (France). Cont. Shelf Res. 17, 1229–1245.
Benitez-Nelson, C.R., 2000. The biogeochemical cycling of phosphorus in marine systems. Earth Sci. Rev. 51, 109–135.
Berner, R.A., 1973. Phosphate removal from sea water by adsorption on volcanogenic ferric oxides. Earth Planet. Sci. Lett. 18 (1), 77–86.
Cha, H.J., Lee, C.B., Kim, B.S., Choi, M.S., Ruttenberg, K.C., 2005. Early diagenetic redistribution and burial of phosphorus in the sediments of the southwestern East Sea (Japan Sea). Mar. Geol. 216, 127–143.
Chai, C., Yu, Z., Song, X., Cao, X., 2006. The status and characteristics of eutrophication in the Yangtze River (Changjiang) Estuary and the adjacent East China Sea, China. Hydrobiologia 563, 313–328.
Chen, C.T.A., 2008. Distributions of nutrients in the East China Sea and the South China Sea connection. J. Oceanogr. 64 (5), 737–751.
Chen, Y.L.L., Chen, H.Y., Gong, G.C., Lin, Y.H., Jan, S., Takahashi, M., 2004. Phytoplankton production during a summer coastal upwelling in the East China Sea. Cont. Shelf Res. 24, 1321–1338.
Chen, Y.L.L., Chen, H.Y., Lee, W.H., Hung, C.C., Wong, G., Kanda, J., 2001. New production in the East China Sea: comparison between well-mixed winter and stratified summer conditions. Cont. Shelf Res. 21, 751–764.
Chen, C.-C., Gong, G.-C., Shiah, F.-K., 2007. Hypoxia in the East China Sea: one of the largest coastal low-oxygen areas in the world. Mar. Environ. Res. 64, 399–408.
Chen, J.J., Lu, S.Y., Zhao, Y.K., Wang, W., Huang, M.S., 2011. Effects of overlying water aeration on phosphorus fractions and alkaline phosphatase activity in surface sediment. J. Environ. Sci. 23, 206–211.
Dunne, E.J., Smith, J., Perkins, D.B., Clark, M.W., Jawitz, J.W., Reddy, K.R., 2007. Phosphorus storages in historically isolated wetland ecosystems and surrounding pasture uplands. Ecol. Eng. 31, 16–28.
Fang, T.H., 2000. Partitioning and behaviour of different forms of phosphorus in the Tanshui Estuary and one of its tributaries, Northern Taiwan. Estuar. Coast. Shelf Sci. 50, 689–701.
Fang, T.H., Chen, J.L., Huh, C.A., 2007. Sedimentary phosphorus species and sedimentation flux in the East China Sea. Cont. Shelf Res. 27 (10–11), 1465–1476.
Fisher, T.R., Carlson, P.R., Barber, R.T., 1982. Sediment nutrient regeneration in three North Carolina estuaries. Estuar. Coast. Shelf Sci. 14, 101–116.
Föllmi, K.B., 1996. The phosphorus cycle, phosphogenesis and marine phosphaterich deposits. Earth Sci. Rev. 40, 55–124.
Giblin, A.E., Hopkinson, C.S., Tucker, J., 1997. Benthic metabolism and nutrient cycling in Boston Harbor, Massachusetts. Estuaries 20, 346–364.
González-Alcaraz, M.N., Egea, C., Jiménez-Cárceles, F.J., Párraga, I., Maria-Cervantes, A., Delgado, M.J., Álvarez-Rogel, J., 2012. Storage of organic carbon, nitrogen and phosphorus in the soil–plant system of *Phragmites australis* stands from a eutrophicated Mediterranean salt marsh. Geoderma 185–186, 61–72.
Gunduz, B., Aydın, F., Aydın, I., Hamamci, C., 2011. Study of phosphorus distribution in coastal surface sediment by sequential extraction procedure (NE Mediterranean Sea, Antalya-Turkey). Microchem. J. 98, 72–76.
Hodell, D.A., Schelske, C.L., 1998. Production, sedimentation, and isotopic composition of organic matter in Lake Ontario. Limnol. Oceanogr. 43 (2), 200–214.
Hong, Y.N., Geng, J.J., Qiao, S., Zhang, Y.Z., Ding, L.L., Wang, X.R., Ren, H., 2010. Phosphorus fractions and matrix-bound phosphine in coastal surface sediments of the Southwest Yellow Sea. J. Hazard. Mater. 181, 556–564.
Huh, C.A., Su, C.C., 1999. Sedimentation dynamics in the East China Sea elucidated from ^{210}Pb, ^{137}Cs and ^{239,240}Pu. Mar. Geol. 160, 183–196.
Huo, S.L., Zan, F.Y., Xi, B.D., Li, Q.Q., Zhang, J.T., 2011. Phosphorus fractionation in different trophic sediments of lakes from different regions, China. J. Environ. Monit. 13, 1088–1095.
Ingall, E., Jahnke, R., 1994. Evidence for enhanced phosphorus regeneration from marine sediments overlain by oxygen depleted waters. Geochim. Cosmochim. Acta 58, 2571–2575.
Ingall, E., Jahnke, R., 1997. Influence of water-column anoxia on the elemental fractionation of carbon and phosphorus during sediment diagenesis. Mar. Geol. 139, 219–229.
Jiang, X., Jin, X.C., Yao, Y., Li, L.H., Wu, F.C., 2008. Effects of biological activity, light, temperature and oxygen on phosphorus release processes at the sediment and water interface of Taihu Lake, China. Water Res. 42 (8–9), 2251–2259.
Kaiser, H.F., 1960. The application of electronic computers to factor analysis. Educ. Psychol. Meas. 20, 141–151.
Kaiserli, A., Voutsa, D., Samara, C., 2002. Phosphorus fractionation in lake sediments — Lakes Volvi and Koronia, N. Greece. Chemosphere 46 (6), 1147–1155.
Keil, R.G., Montluçon, D.B., Prahl, F.G., Hedges, J.I., 1994. Sorptive preservation of labile organic matter in marine sediments. Nature 370, 549–552.
Li, D.J., Daler, D., 2004. Ocean pollution from land-based sources: East China Sea, China. Ambio 33 (1–2), 107–113.
Li, X.X., Bianchi, T.S., Allison, M.A., Chapman, P., Mitra, S., Zhang, Z.R., Yang, G.P., Yu, Z.G., 2012. Composition, abundance and age of total organic carbon in surface sediments from the inner shelf of the East China Sea. Mar. Chem. 145–147, 37–52.
Li, J., Glibert, P.M., Zhou, M.J., 2010. Temporal and spatial variability in nitrogen uptake kinetics during harmful dinoflagellate blooms in the East China Sea. Harmful Algae 9, 531–539.
Li, H.M., Tang, H.J., Shi, X.Y., Zhang, C.S., Wang, X.L., 2014. Increased nutrient loads from the Changjiang (Yangtze) River have led to increased Harmful Algal Blooms. Harmful Algae 39, 92–101.
Liu, K.-K., Yan, W.J., Lee, H.-J., Chao, S.-Y., Gong, G.-C., Yeh, T.-Y., 2015. Impacts of increasing dissolved inorganic nitrogen discharged from Changjiang on primary production and seafloor oxygen demand in the East China Sea from 1970 to 2002. J. Mar. Syst. 141, 200–217.

Liu, Z.L., Yue, C.H., Ning, X.R., Shi, J.X., Cai, Y.M., 2001. Bacterioplankton production in dilution zone of the Changjiang (Yangtze River) Estuary. Acta Oceanol. Sin. 20 (1), 131–139.
Liu, S.M., Zhang, W.G., He, Q., Li, D.J., Liu, H., Yu, L.Z., 2010. Magnetic properties of East China Sea shelf sediments off the Yangtze Estuary: influence of provenance and particle size. Geomorphology 119 (3–4), 212–220.
Liu, S.M., Zhang, J., Li, D.J., 2004. Phosphorus cycling in sediments of the Bohai and Yellow Seas. Estuar. Coast. Shelf Sci. 59, 209–218.
Loska, K., Wiechuła, D., 2003. Application of principal component analysis for the estimation of source of heavy metal contamination in surface sediments from the Rybnik Reservoir. Chemosphere 51, 723–733.
Lui, H.K., Chen, C.T.A., 2011. Shifts in limiting nutrients in an estuary caused by mixing and biological activity. Limnol. Oceanogr. 56, 989–998.
Łukawska-Matuszewska, K., Bolałek, J., 2008. Spatial distribution of phosphorus forms in sediments in the Gulf of Gdańsk (southern Baltic Sea). Cont. Shelf Res. 28, 977–990.
Mayer, L.M., 1994. Surface area control of organic carbon accumulation in continental shelf sediments. Geochim. Cosmochim. Acta 58, 1271–1284.
Meng, J., Yao, P., Yu, Z.G., Bianchi, T.S., Zhao, B., Pan, H.H., Li, D., 2014. Speciation, bioavailability and preservation of phosphorus in surface sediments of the Changjiang Estuary and adjacent East China Sea inner shelf. Estuar. Coast. Shelf Sci. 144, 27–38.
Meng, J., Yao, P., Bianchi, T.S., Li, D., Zhao, B., Xu, B.C., Yu, Z.G., 2015a. Detrital phosphorus as a proxy of flooding events in the Changjiang River Basin. Sci. Total Environ. 517, 22–30.
Meng, J., Yu, Z.G., Yao, Q.Z., Bianchi, T.S., Paytan, A., Zhao, B., Pan, H.H., Yao, P., 2015b. Distribution, mixing behavior, and transformation of dissolved inorganic phosphorus and suspended particulate phosphorus along a salinity gradient in the Changjiang Estuary. Mar. Chem. 168, 124–134.
Meyers, P.A., 2003. Applications of organic geochemistry to paleolimnological reconstructions: a summary of examples from the Laurentian Great Lakes. Org. Geochem. 34 (2), 261–289.
Milliman, J.D., Meade, R.H., 1983. World-wide delivery of sediment to the oceans. J. Geol. 91, 1–21.
Milliman, J.D., Shen, H.T., Yang, Z.S., Meade, R.H., 1985. Transport and deposition of river sediment in the Changjiang estuary and adjacent continental shelf. Cont. Shelf Res. 4, 37–45.
Morrison, D., 1967. Multivariate Statistical Methods. McGraw-Hill, New York.
Rabouille, C., Conley, D.J., Dai, M.H., Cai, W.J., Chen, C.T.A., Lansard, B., Green, R., Yin, K., Harrison, P.J., Dagg, M., McKee, B., 2008. Comparison of hypoxia among four river-dominated ocean margins: the Changjiang (Yangtze), Mississippi, Pearl, and Rhône rivers. Cont. Shelf Res. 28 (12), 1527–1537.
Redfield, A.C., Ketchum, B.H., Richards, F.A., 1963. The Influence of Organisms on the Composition of Sea-water. In: Hill, M.N. (Ed.)The Sea vol. 2. Interscience Publisher, New York, pp. 26–77.
Reynolds, C.S., 1976. Succession and vertical distribution of phytoplankton in response to thermal stratification in a lowland mere, with special reference to nutrient availability. J. Ecol. 64, 529–551.
Ruban, V., López-Sánchez, J.F., Pardo, P., Rauret, G., Muntau, H., Quevauviller, P., 2001. Harmonized protocol and certified reference material for the determination of extractable contents of phosphorus in freshwater sediments — a synthesis of recent works. Fresenius J. Anal. Chem. 370, 224–228.
Ruttenberg, K.C., 1992. Development of a sequential extraction technique for different forms of phosphorus in marine sediments. Limnol. Oceanogr. 37, 1460–1482.
Ruttenberg, K.C., Berner, R.A., 1993. Authigenic apatite formation and burial in sediments from non-upwelling, continental margin environments. Geochim. Cosmochim. Acta 57 (5), 991–1007.
Ruttenberg, K.C., Goñi, M.A., 1997. Phosphorus distribution, C:N:P ratios, and $\delta^{13}C_{OC}$ in arctic, temperate, and tropical coastal sediments: tools for characterizing bulk sedimentary organic matter. Mar. Geol. 139, 123–145.
Rydin, E., 2000. Potentially mobile phosphorus in Lake Erken sediment. Water Res. 34, 2037–2042.
Sagher, A., Harris, R.F., Armstrong, D.E., 1975. Biological availability of sediment phosphorus to microorganisms. Technical Report. Wisconsin Water Resources Center, Madison (57 pp.).
Samadi-Maybodi, A., Taheri Saffar, H., Khodadoust, S., Nasrollahzadeh Saravi, H., Najafpour, S., 2013. Study on different forms and phosphorus distribution in the coastal surface sediments of Southern Caspian Sea by using UV–Vis spectrophotometery. Spectrochim. Acta A Mol. Biomol. Spectrosc. 113, 67–71.
Sardans, J., Rivas-Ubach, A., Peñuelas, J., 2012. The elemental stoichiometry of aquatic and terrestrial ecosystems and its relationships with organismic lifestyle and ecosystem structure and function: a review and perspectives. Biogeochemistry 111, 1–39.
Schelske, C.L., Hodell, D.A., 1995. Using carbon isotopes of bulk sedimentary organic matter to reconstruct the history of nutrient loading and eutrophication in Lake Erie. Limnol. Oceanogr. 40 (5), 918–929.
Schelske, C.L., Robbins, J.A., Gardner, W.S., Conley, D.J., Bourbonniere, R.A., 1988. Sediment record of biogeochemical responses to anthropogenic perturbations of nutrient cycles in Lake-Ontario. Can. J. Fish. Aquat. Sci. 45 (7), 1291–1303.
Schelske, C.L., Stoermer, E.F., Kenney, W.F., 2006. Historic low level phosphorus enrichment in the Great Lakes inferred from biogenic silica accumulation in sediments. Limnol. Oceanogr. 51 (1), 728–748.
Schenau, S.J., de Lange, G.J., 2001. Phosphorus regeneration vs. burial in sediments of the Arabian Sea. Mar. Chem. 75, 201–217.
Sekula-Wood, E., Benitez-Nelson, C.R., Bennett, M.A., Thunell, R., 2012. Magnitude and composition of sinking particulate phosphorus fluxes in Santa Barbara Basin, California. Glob. Biogeochem. Cycles 26, 1–15.
Shao, X.X., Liang, X.Q., Wu, M., Gu, B.H., Li, W.H., Sheng, X.C., Wang, S.X., 2014. Influences of sediment properties and macrophytes on phosphorous speciation in the intertidal marsh. Environ. Sci. Pollut. Res. 21 (17), 10432–10441.
Shen, H.T., 2001. Material Flux of the Changjiang Estuary. Ocean Press, Beijing (176 pp. (in Chinese)).
Shepard, F.P., 1954. Nomenclature based on sand–silt–clay ratios. J. Sediment. Petrol. 24, 151–158.
Song, J.M., 2010. Biogeochemical Processes of Biogenic Elements in China Marginal Seas. Springer, Berlin Heidelberg (676 pp.).
Song, G.D., Liu, S.M., 2015. Phosphorus speciation and distribution in surface sediments of the Yellow Sea and East China Sea and potential impacts on ecosystem. Acta Oceanol. Sin. 34 (4), 84–91.
Su, C.C., 2000. Sedimentation Dynamics in the East China Sea: A Multitracer Approach (Ph.D. Thesis) Institute of Oceanography, National Taiwan University, Taiwan.
Su, C.C., Huh, C.A., 2002. ^{210}Pb, ^{137}Cs and ^{239,240}Pu in the East China Sea sediments: sources, pathways and budgets of sediments and radionuclides. Mar. Geol. 183, 163–178.
Van Raaphorst, W., Kloosterhuis, H.T., 1994. Phosphate sorption in superficial intertidal sediments. Mar. Chem. 48 (1), 1–16.
Wang, B.D., 2009. Hydromorphological mechanisms leading to hypoxia off the Changjiang estuary. Mar. Environ. Res. 67 (1), 53–58.
Wang, J.Y., Ding, Y.H., 2008. Climatic characteristics of rainy seasons in China. Chin. J. Atmos. Sci. 32 (1), 1–13 (In Chinese with English abstract).
Wang, Y.P., Law, R.M., Pak, B., 2010. A global model of carbon, nitrogen and phosphorus cycles for the terrestrial biosphere. Biogeosciences 7, 2261–2282.
Wang, B.D., Wei, Q.S., Chen, J.F., Xie, L.P., 2012. Annual cycle of hypoxia off the Changjiang (Yangtze River) Estuary. Mar. Environ. Res. 77, 1–5.
Wei, H., He, Y.C., Li, Q.J., Liu, Z.Y., Wang, H.T., 2007. Summer hypoxia adjacent to the Changjiang estuary. J. Mar. Syst. 67, 292–303.
Williams, J.D.H., Shear, H., Thomas, R.L., 1980. Availability to *Scenedesmus quadricauda* of different forms of phosphorus in sedimentary materials from the Great Lakes. Limnol. Oceanogr. 25 (1), 1–11.
Xing, Q.G., Tosi, L., Braga, F., Gao, X.L., Gao, M., 2015. Interpreting the progressive eutrophication behind the world's largest macroalgal blooms with water quality and ocean color data. Nat. Hazards 78 (1), 7–21.
Xing, L., Zhang, H.L., Yuan, Z.N., Sun, Y., Zhao, M.X., 2011. Terrestrial and marine biomarker estimates of organic matter sources and distributions in surface sediments from the East China Sea shelf. Cont. Shelf Res. 31, 1106–1115.
Yang, B., Cao, L., Liu, S.M., Zhang, G.S., 2015. Biogeochemistry of bulk organic matter and biogenic elements in surface sediments of the Yangtze River Estuary and adjacent sea. Mar. Pollut. Bull. 96, 471–484.
Yu, Y., Song, J.M., Li, X.G., Yuan, H.M., Li, N., 2012. Distribution, sources and budgets of particulate phosphorus and nitrogen in the East China Sea. Cont. Shelf Res. 43, 142–155.
Yu, Y., Song, J.M., Li, X.G., Yuan, H.M., Li, N., Duan, L.Q., 2011. Distributions and environmental implications of the phosphorus forms in the surface sediments from the Changjiang Estuary. Adv. Earth Sci. 26 (8), 870–880.
Yu, Y., Song, J.M., Li, X.G., Yuan, H.M., Li, N., Duan, L.Q., 2013. Environmental significance of biogenic elements in surface sediments of the Changjiang Estuary and its adjacent areas. J. Environ. Sci. 25 (11), 2185–2195.
Zabel, M., Dahmke, A., Schulz, H.D., 1998. Reginal distribution of diffusive phosphate and silicate fluxes through the sediment–water interface: the eastern south Atlantic. Deep-Sea Res. I 45, 277–300.
Zhang, R.Y., Wu, F.C., Liu, C.Q., Fu, P.Q., Li, W., Wang, L.Y., Liao, H.Q., Guo, J.Y., 2008. Characteristics of organic phosphorus fractions in different trophic sediments of lakes from the middle and lower reaches of Yangtze River region and Southwestern Plateau, China. Environ. Pollut. 152, 366–372.
Zhou, F.X., Gao, X.L., Zhuang, W., Zhang, J.F., Li, P.M., 2015. The impact of rivers on the Chl a concentrations in coastal surface waters of the Laizhou Bay. Mar. Environ. Sci. 34 (2), 184–189 (In Chinese with English abstract).
Zhou, Q., Gibson, C.E., Zhu, Y., 2001. Evaluation of phosphorus bioavailability in sediments of three contrasting lakes in China and the UK. Chemosphere 42, 221–225.
Zhou, M.J., Shen, Z.L., Yu, R.C., 2008. Responses of a coastal phytoplankton community to increased nutrient input from the Changjiang (Yangtze) River. Cont. Shelf Res. 28 (12), 1483–1489.
Zhu, C., Wang, Z.H., Xue, B., Yu, P.S., Pan, J.M., Wagner, T., Pancost, R.D., 2011. Characterizing the depositional settings for sedimentary organic matter distributions in the Lower Yangtze River-East China Sea Shelf system. Estuar. Coast. Shelf Sci. 93 (3), 182–191.
Zhuang, W., Gao, X.L., Zhang, Y., Xing, Q.G., Tosi, L., Qin, S., 2014. Geochemical characteristics of phosphorus in surface sediments of two major Chinese mariculture areas: the Laizhou Bay and the coastal waters of the Zhangzi Island. Mar. Pollut. Bull. 83 (1), 343–351.